JOURNAL OF MATERIALS SCIENCE 31 (1996) 6403–6407

Interface characterization of a β-SiC whisker–Al composite

Z. R. LIU, D. Z. WANG, C. K. YAO
National Defence Key Laboratory for Precision Hot-working, School of Materials Science and Engineering, Harbin Institute of Technology, Harbin 150001, People's Republic of China
J. F. MAO, D. X. LI
Institute of Metal Research Academia Sinica, Shenyang 110015, People's Republic of China

The nature of the interface, the orientation relationship of β-SiC whisker (β-SiC_w)–Al combination, and the misfit dislocation structures at the β-SiC_w–Al interfaces in a β-SiC_w–Al composite have been observed by a high-resolution transmission electron microscopy (HRTEM). It was shown that quite a good bonding between the whisker and the aluminium was achieved due largely to the lattice match between SiC and aluminium at the interfaces. The orientation relationship between the whisker and the aluminium was $\{0\,0\,2\}_{SiC} \parallel \{1\,1\,1\}_{Al}$; $\langle 1\,1\,0\rangle_{SiC} \parallel \langle 1\,1\,0\rangle_{Al}$. The interface was clean, faceted and semicoherent. The misfit dislocation cores were located in the whisker side away from the β-SiC_w–Al interfaces.

1. Introduction

In recent years, interfaces in metal matrix composites have received much attention because the mechanical properties of a metal-matrix composite are strongly influenced by the characterization of the interface between the reinforcement and the matrix. This interface controls the efficiency of the load transfer between the matrix and the reinforcement. Previous investigations concerning interface characterization in an SiC–Al system can be classified mainly into three groups, according to:

1. the nature of the interface, including the mechanism of the SiC–Al bonding and the composition and phase analyses of the interface [1–11];
2. the crystallographic orientations of SiC–Al combination [12–16];
3. the interfacial bonding strength and the interfacial energy [9, 11, 17–20]

The interface characterization for an SiC–Al system depends on a variety of factors, such as:

1. the structure of SiC [12, 13];
2. the nature of the SiC surface [4, 21–23];
3. the composition of the aluminium alloy [24, 25];
4. the fabrication technique and processing [12–16];
5. the heat-treatment conditions applied to the composite [5, 26].

Available results show that there are reaction products such as Al_4C_3 on the SiC–Al interface [3, 7]. Intermetallic particles such as Mg_2Si and $FeSiAl_5$ and precipitates [4–8, 27] can also be observed. On the other hand, the interface is clean in some composites [13, 16], i.e. the interface is simply formed by two surfaces of SiC and Al.

A common point of view is that the bonding strength between SiC and aluminium is usually quite good. An available model proposed by Flom and Arsenault [18] predicts a lower bound interface strength in an SiC–6061Al composite to be 1690 MPa. The work of Li *et al.* [28] considered that the bond strength between SiC and aluminium could possibly be two to three times stronger than the bond between aluminium and aluminium. On the other hand, measurements of the interfacial strength in SiC–Al composites indicate that the values of interfacial strength are about 1.5 times [20], and 3 times [19] as high as the UTS of the composites. However, understanding of the interface bonding mechanism is still poor. A mechanism concerning the interface between SiC and aluminium was proposed based on scanning Auger microprobe analysis and STEM analysis in which there is diffusion of aluminium into SiC, and the diffusion bonding results in a high-strength bond [1]. Inconsistent with this result, one conclusion can be drawn from the investigation of Cao *et al.* [2] that the interaction between SiC and aluminium (including the interface reaction and diffusion) has only taken place over a range of 50 nm; silicon and carbon appear not to diffuse into the aluminium matrix through the interface, and aluminium appears not to diffuse into the SiC whisker [2], consistent with the recent work of Arsenault [13]. In addition to the five factors affecting the interface characterization, as mentioned above, this difference may also be explained by the following reasons: (1) the SiC surface has a zigzag shape which may result in an overlap of SiC and aluminium at the interface in TEM specimens; (2) the spatial resolution of the energy-dispersive X-ray analysis is about 30 nm, which is equivalent to the width of 120 interplanar spacings of $(1\,1\,1)_{SiC}$, which will certainly have an effect on the results of the composition analysis of the interface if the interface is studied from an atomic viewpoint.

0022–2461

Previous studies also show that as long as the matrix is in the liquid state during preparation of the composite, a consistent result is obtained by different research groups, i.e. there are orientation relationships for SiC–Al combination [13, 14, 16]. On the other hand, when the matrix is in the solid state, inconsistent results are obtained, i.e. there are orientation relationships for some SiC–Al composites [16] but, there is no orientation relationship of any kind for other SiC–Al composites [15, 16]. The orientation relationships between the SiC and aluminium in α-SiC particulate-6061Al composites have been reported by several research groups [13–16], but few papers on this aspect in β-SiC whisker–Al composites have been published. In addition, understanding of the misfit dislocation structures at interfaces in SiC–Al composites is still poor, however, the plastic relaxation of thermal misfit stress depends directly on the dislocations at the interface.

The purpose of the present work is to determine in greater detail the interface including the interfacial nature, the mechanism of SiC–Al bonding, the orientation relationship and the misfit dislocation structures in a β-SiC_w–Al composite.

2. Experimental procedure

The reinforcement used in this work was the β-SiC whisker obtained from Tokai Carbon Co. Ltd of Japan. The matrix was commercial pure (99.75%) aluminium. A 22 vol % β-SiC_w–Al composite was fabricated by a squeeze-casting method. The specimens, 5 mm diameter and 0.3 mm thick, were cut from the as-cast composite by spark erosion. Subsequently, they were thinned by grinding and dimpling and were further thinned by ion milling with a 4.5 kV argon ion beam under an angle of 7°.

The HRTEM observation was performed in a JEM 2000EX–II high-resolution electron microscope operated at 200 kV. The fracture surface of the composite was *in situ* examined using a Philips CM_{12} scanning/transmission electron microscopy.

3. Results and discussion

3.1. The nature of the interface and the mechanism of SiC–Al bonding

Fig. 1a and b shows the HRTEM morphologies of β-SiC_w–Al interfaces between aluminium and the transverse and longitudinal sections of β-SiC whisker, respectively. There was no interfacial phase at the interfaces.

Fig. 2a shows a high-resolution electron micrograph of a β-SiC_w–Al interface. A high density of atomic steps with no reaction layer, void or amorphous phase can be found at the interface, i.e. the interface is clean and faceted. A lattice match between SiC and aluminium is formed. The fracture surface of the composite is shown in Fig. 3. A layer of aluminium can be found adhering to the SiC whisker exposed on the fracture surface (further details about the analysis of the fracture surface are presented elsewhere [29]). This indicates that a high interfacial bond strength is obtained. So it can be concluded that quite a good bonding between the SiC and aluminium is achieved due to the direct lattice match between SiC and aluminium.

3.2. The orientation relationship

Fig. 2b and c shows the electron diffraction patterns of SiC and aluminium in Fig. 2a, respectively. An orientation relationship between SiC and aluminium can

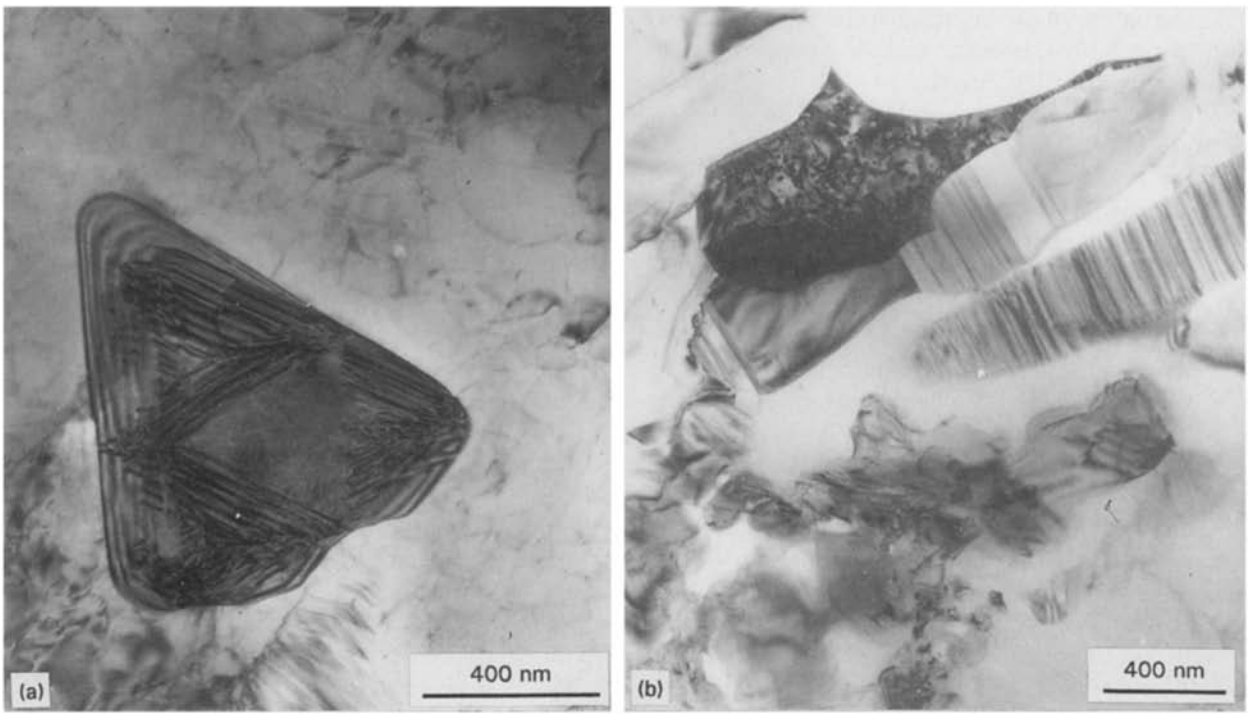

Figure 1 HRTEM morphologies showing β-SiC_w–Al interfaces between aluminium and (a) transverse and (b) longitudinal sections of β-SiC whisker.

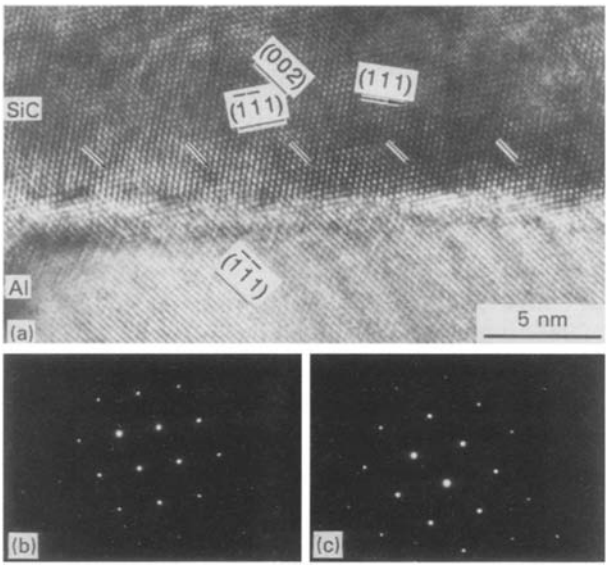

Figure 2 (a) HRTEM image of β-SiC_w–Al interface: (b) and (c) are the electron diffraction patterns for the whisker and the aluminium, respectively, in (a) (pole [$\bar{1}$ 1 0]).

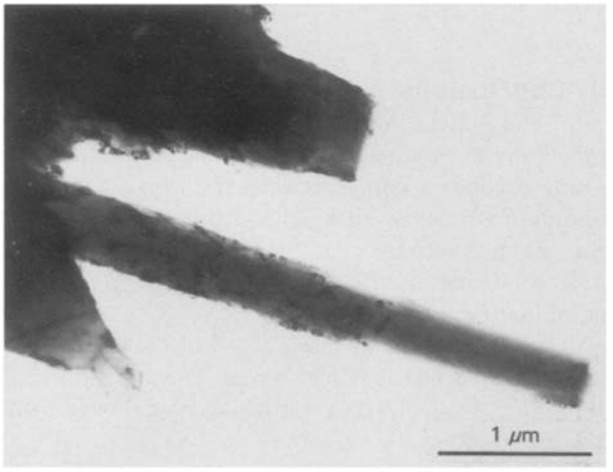

Figure 3 TEM image of the fracture surface of β-SiC_w–Al composite.

be obtained: $\{0\,0\,2\}_{SiC} \parallel \{1\,1\,1\}_{Al}$; $\langle 1\,1\,0\rangle_{SiC} \parallel \langle 1\,1\,0\rangle_{Al}$, which can be more clearly shown in Fig. 4, which is a schematic representation of Fig. 2a, i.e. the projection of the SiC lattice and the aluminium lattice on $(\bar{1}\,1\,0)_{SiC}$ and $(\bar{1}\,1\,0)_{Al}$ planes, respectively. The crystallographic orientation between SiC and aluminium is $(0\,0\,2)SiC \parallel (\bar{1}\,\bar{1}\,1)_{Al}$; $\langle 0\,\bar{1}\,1\rangle_{SiC} \parallel \langle \bar{1}\,\bar{1}\,0\rangle_{Al}$. In Fig. 4 the angle between $(1\,1\,1)_{Al}$ and $(\bar{1}\,\bar{1}\,1)_{SiC}$ planes is 15.78°. This can be further proved by Fig. 5, which shows the HRTEM image of the SiC–Al interface under different directions of the electron beam at the same site in Fig. 2a. The angle between $(1\,1\,1)_{Al}$ and $(\bar{1}\,\bar{1}\,1)_{SiC}$ planes is about 15° measured from the high-resolution image, with a good agreement with the calculated value. The interface between $(1\,1\,1)_{Al}$ and $(\bar{1}\,\bar{1}\,1)_{SiC}$ planes is incoherent and no regular interfacial dislocations can be found. According to Fig. 4, the following orientation relationship can also be deduced: $\{1\,1\,1\}_{SiC} \parallel \{0\,0\,2\}_{Al}$; $\langle 1\,1\,0\rangle_{SiC} \parallel \langle 1\,1\,0\rangle_{Al}$.

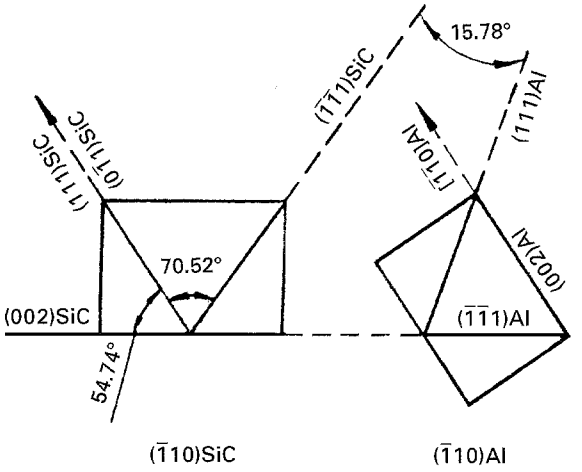

Figure 4 Schematic drawing of the orientation relationship between SiC and aluminium in Fig. 2a.

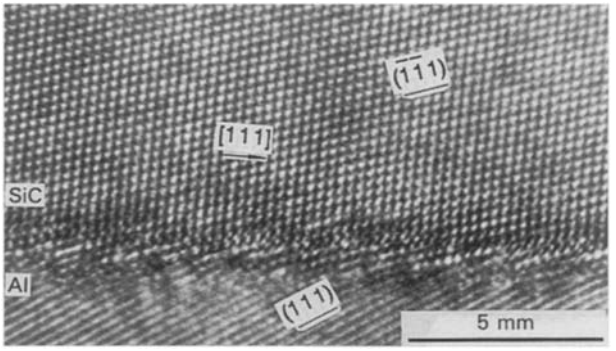

Figure 5 HRTEM image of the β-SiC_w–Al interface.

The orientation relationship may be analysed as follows using the schematic drawing in Fig. 6, which shows the crystalline lattice pattern of the side surface of the β-SiC whisker in contact with the aluminium in Fig. 2a. The angle between the $(\bar{1}\,\bar{1}\,1)$ plane and the [1 1 1] direction, i.e. the growth axis of β-SiC whisker, is 9.74°. The side surface of SiC consists of atomic steps, which are mainly composed of three crystallographic planes, with indices $(\bar{1}\,\bar{1}\,1)$, (1 1 1) and (0 0 2), respectively, as shown in Fig. 6. Those steps will become favourable sites for molten aluminium to nucleate. The closely packed plane and the closely packed direction of aluminium are $\{1\,1\,1\}$ and $\langle 1\,1\,0\rangle$, respectively. In order to decrease the free energy during the process of the nucleation and growth of molten aluminium, the highest growth rate along the $\{1\,1\,1\}_{Al}$ plane and the $\langle 1\,1\,0\rangle_{Al}$ direction can be achieved [30]. In order to form the preferred orientation relationship in the β-SiC_w–Al combination, the growth rate will also obey the law of the lowest free energy to choose which lattice plane and lattice direction of SiC to match to $\{1\,1\,1\}_{Al}$ and $\langle 1\,1\,0\rangle_{Al}$, due to the difference in lattice parameter between SiC and aluminium, i.e. the lowest mismatch should be achieved from the match between SiC and aluminium to reduce the interfacial strain energy. The interplanar spacing of $(\bar{1}\,\bar{1}\,1)_{Al}$ is 0.2338 nm, and the interplaner spacings of SiC corresponding to $(\bar{1}\,\bar{1}\,1)$, (1 1 1) and (0 0 2) are 0.251, 0.251 and 0.217 nm, respectively. The difference

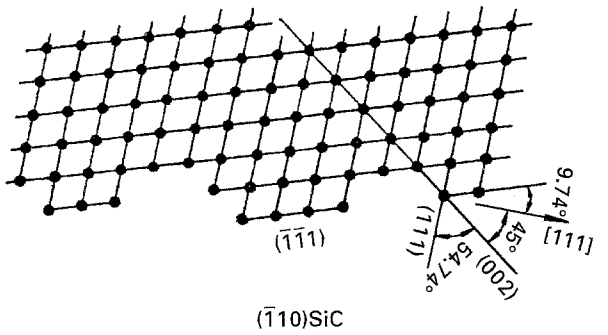

Figure 6 Schematic illustration of the structure of the side surface of β-SiC whisker: (●) SiC.

in interplanar spacing, Δ between $(\bar{1}\,\bar{1}\,1)_{Al}$ and $(\bar{1}\,\bar{1}\,1)_{SiC}$, $(1\,1\,1)_{SiC}$ and $(0\,0\,2)_{SiC}$ can be given by

$$\Delta = d_{SiC} - d_{Al} \quad (1)$$

i.e. 0.172, 0.172 and −0.168, respectively. The difference in the interplanar spacings between $(\bar{1}\,\bar{1}\,1)_{Al}$ and $(0\,0\,2)_{SiC}$ is the lowest, and a low interfacial dislocation density would be generated at the interface, i.e. the interfacial strain energy might be the lowest. Thus, as far as energy is concerned it is favourable to choose $(0\,0\,2)_{SiC}$ as the substrate plane for molten aluminium to nucleate. This may be the reason why the $(\bar{1}\,\bar{1}\,1)_{Al}$ planes are not bonded parallel to the $(1\,1\,1)_{SiC}$ planes, even though they have a stacking similar to the $(1\,1\,1)_{SiC}$ planes. This appears to be similar to the result reported by Arsenault [13], in an α-SiC particulate–Al composite, who found the $(1\,1\,2)_{Al}$ planes instead of $(1\,1\,1)_{Al}$ planes bonded parallel to the $(0\,0\,0\,1)_{SiC}$ planes.

3.3. Dislocation structures at the β-SiC_w–Al interface

In Fig. 2a the interfacial misfit dislocations are clearly visible. The core-like feature of the dislocations clearly indicates that the dislocation lines are parallel to the electron beam, i.e. $[\bar{1}\,1\,0]$ direction. The strain field of the dislocation appears to be largely limited to the whisker side of the interface. The number of the $(0\,0\,2)_{SiC}$ lattice planes between two neighbouring edge dislocations is about 14. The average value of the spacings between the dislocations measured from the high-resolution image is about 3.138 nm. The interface between SiC and aluminium is semicoherent.

The lattice plane spacings of $(0\,0\,2)_{SiC}$ and $(1\,1\,1)_{Al}$ are incommensurate. However, owing to relaxations along the interface, an epitaxial fit is achieved at the β-SiC_w–Al interface. The mismatch between $(1\,1\,1)_{Al}$ and $(0\,0\,2)_{SiC}$ is accommodated by localized misfit dislocations in the whisker. The distance between misfit dislocations, D, can be calculated from

$$D = d_{Al}d_{SiC}/(d_{Al} - d_{SiC}) \quad (2)$$

where D_{Al} and D_{SiC} are the interplanar distances for aluminium and SiC, respectively, The interplanar distances of (1 1 1) planes in aluminium and (0 0 2) planes in SiC are 0.2338 and 0.217 nm, respectively. From calculation, $D = 3.02$ nm, which is about 14 times greater than the interplanar distance of (0 0 2) planes in SiC, with good agreement to the value measured from the high-resolution image.

A common observation made for most metal-oxide interfaces, such as Nb–Al_2O_3 [31], Ag–MgO [32], Nb–MgO [33], Cu–MgO and Pd–MgO [34] is that the misfit dislocation cores are located in the metal side away from the interface, and the "stand off" distance varies from system to system, ranging from one to three interplanar spacings. In α-SiC particulate–Aluminium composites no regular dislocation distribution and no distinctive periodic pattern have been observed [13, 16]. Inconsistent with these observations, in the present work the edge dislocation cores are located in the SiC side (not in the metallic aluminium side) away from the β-SiC_w–Al interface. It is clear that the deformation of SiC is difficult owing to its high elastic modulus, so the observation that the mismatch can be accommodated by misfit dislocation in the whisker probably indicates that the formation of this kind of dislocation structure is favourable from the free-energy viewpoint, and in order to form the half atomic plane of the misfit dislocation, a short distance diffusion for SiC may occur in the surface of the whisker at high temperature.

4. Conclusions

1. The β-SiC_w–Al interface in the β-SiC_w–Al composite made by squeeze casting is clean and faceted. Quite a good bonding between the whisker and the aluminium is achieved by the lattice match between SiC and aluminium.
2. An orientation relationship in the β-SiC_w–Al combination is:
$\{0\,0\,2\}_{SiC} \parallel \{1\,1\,1\}_{Al}$; $\langle 1\,1\,0\rangle_{SiC} \parallel \langle 1\,1\,0\rangle_{Al}$.
3. The interface is semicoherent. The misfit dislocation cores are located in the whisker side away from the interface.

Acknowledgement

This work was supported by National Nature Science Foundation of China, no. 59381002.

References

1. R. J. ARSENAULT and C. S. PANDE, *Scripta Metall.* **18** (1984) 1131.
2. L. CAO, L. GENG, C. K. YAO and T. C. LEI, *ibid.* **23** (1989) 227.
3. F. BONOLLO, R. GUERRIERO, E. SENTIMENTI, I. TANGERINI and W. L. YANG, *Mater. Sci. Eng.* **A144** (1991) 303.
4. H. RIBES, R. DA SILVA, M. SUERY and T. BRETHEAU, *Mater. Sci. Technol.* **6** (1990) 621.
5. C. J. MAHON, J. M. HOWE and A. K. VASUDEVAN, *Acta. Metall. Mater.* **38** (1990) 1503.
6. G. M. JANOWSKI and B. J. PLETKA, *Mater. Sci. Eng.* **A129** (1990) 65.
7. S. R. NUTT and R. W. CARPENTER, *ibid.* **75** (1985) 169.
8. B. R. HENRIKSEN and T. E. JOHNSEN, *Mater. Sci. Technol.* **6** (1990) 857.
9. P. K. ROHATGI, S. RAY, R. ASTHANA and C. S. NARENDRANATH, *Mater. Sci. Eng.* **A162** (1993) 163.
10. E. A. FEEST, *Composites* **25** (1994) 75.

11. K. S. FOO, W. M. BANKS, A. J. CRAVEN and A. HENDRY, *ibid.* **25** (1994) 677.
12. L. GENG and C. K. YAO, *J. Mater. Sci. Lett.* **14** (1995) 606.
13. R. J. ARSENAULT, *Composites* **25** (1994) 540.
14. A. H. CARIM, *Mater. Lett.* **12** (1991) 153.
15. V. RADMILOVIC, G. THOMAS and S. K. DAS, *Mater. Sci. Eng.* **A132** (1991) 171.
16. M. VAN DEN BURG and J. TH. M. DE HOSSON, *Acta Metall. Mater.* **40** (1992) s281.
17. B. K. RAO and P. JENA, *Appl. Phys. Lett.* **57** (1990) 2308.
18. Y. FLOM and R. J. ARSENAULT, *Mater. Sci. Eng.* **77** (1986) 191.
19. Y. H. TENG and J. D. BOYD, *Composites* **25** (1994) 906.
20. J. C. LEE and K. N. SUBRAMANIAN, *J. Mater. Sci.* **27** (1992) 5453.
21. H. RIBES and M. SUERY, *Script Metall.* **23** (1989) 705.
22. L. SALVO, M. SUERY, J. G. LEGOUX and G. L'ESPERANCE, *Mater. Sci. Eng.* **A135** (1991) 129.
23. A. E. HUGHES, M. M. HEDGES and B. A. SEXTON, *J. Mater. Sci.* **25** (1990) 4856.
24. B. R. HENRIKSEN, *Composites* **31** (1990) 333.
25. N. DAHL and T. E. JOHNSEN, *Mater. Sci. Eng.* **A135** (1991) 151.
26. M. STRANGEWOOD, C. A. HIPPSLEY and J. J. LEWANDOWSKI, *Scripta Metall. Mater.* **24** (1990) 1483.
27. J. J. LEWANDOWSKI, C. LIU and W. H. HUNT, *Mater. Sci. Eng.* **A107** (1989) 241.
28. S. LI, R. J. ARSENAULT and P. JENA, *J. Appl. Phys.* **64** (1988) 6246.
29. Z. R. LIU, D. Z. WANG, C. K. YAO, J. LIU and L. GENG, *Mater. Sci. Eng.* **A189** (1994) 235.
30. N. B. MIN, "Physical basics of the growth of crystals" (Shanghai Science and Technology Publishing House, Shanghai, China, 1982) p. 283.
31. J. MAYER, G. GUTEKUNST, G. MOBUS, J. DURA, C. P. FLYNN and M. RÜHLE, *Acta Metall. Mater.* **40** (1992) s217.
32. A. TRAMPERT, F. ERNST, C. P. FLYNN, H. F. FISCHMEISTER and M. RÜHLE, *ibid.* **40** (1992) s227.
33. D. X. LI, P. PIROUZ, A. H. HEUER, S. YADAVALLI and C. P. FLYNN, *Acta Metall. Mater.* **40** (1992) s237.
34. P. LU and F. COSANDEY, *ibid.* **40** (1992) s259.

Received 9 January
and accepted 18 March 1996